Rapid Communications

Effect of density on microwave-induced resistance oscillations in back-gated GaAs quantum wells

X. Fu,[1] M. D. Borisov,[1] M. A. Zudov,[1,*] Q. Qian,[2] J. D. Watson,[2,†] and M. J. Manfra[2,3,4]
[1]School of Physics and Astronomy, University of Minnesota, Minneapolis, Minnesota 55455, USA
[2]Department of Physics and Astronomy and Birck Nanotechnology Center, Purdue University, West Lafayette, Indiana 47907, USA
[3]Station Q Purdue, Purdue University, West Lafayette, Indiana 47907, USA
[4]School of Materials Engineering and School of Electrical and Computer Engineering, Purdue University, West Lafayette, Indiana 47907, USA

(Received 7 November 2017; revised manuscript received 9 August 2018; published 17 September 2018)

We report on microwave-induced resistance oscillations (MIROs) in a tunable-density 30-nm-wide GaAs/AlGaAs quantum well. We find that the MIRO amplitude increases dramatically with carrier density. Our analysis shows that the anticipated increase in the effective microwave power and quantum lifetime with density is *not* sufficient to explain the observed growth of the amplitude. We further observe that the fundamental oscillation extrema move towards cyclotron resonance with increasing density, which also contradicts theoretical predictions. These findings reveal that the density dependence is not properly captured by existing theories, calling for further studies.

DOI: 10.1103/PhysRevB.98.121303

Microwave-induced resistance oscillations (MIROs) appear in a two-dimensional (2D) electron gas (2DEG) [1–3] (or a 2D hole gas [4,5]) subjected to low temperature T, weak magnetic field B, and microwave radiation of frequency $f = \omega/2\pi$. It is well established experimentally that MIROs originate from the bulk of the 2DEG [6–16]. Theoretically, microwave photoresistance δR due to MIROs can be described by [17–19]

$$\frac{\delta R(\epsilon)}{R_0} = -2\pi\epsilon\lambda^2\mathcal{P}\eta\sin 2\pi\epsilon. \qquad (1)$$

Here, R_0 is the resistance at $B = 0$, $\epsilon = \omega/\omega_c$, $\omega_c = eB/m^\star$ is the cyclotron frequency of the charge carrier with the effective mass $m^\star$, $\lambda = \exp(-\epsilon/2f\tau_q)$ is the Dingle factor, τ_q is the quantum lifetime, $\mathcal{P}$ is the effective microwave power, and η is the dimensionless parameter (discussed later in detail) which depends on the disorder characteristics and the inelastic relaxation. The above expression was obtained assuming $2\pi k_B T \gg \hbar\omega$ and is accurate away from the cyclotron resonance ($2\pi\epsilon \gg 1$), when the microwave power is not too high ($\mathcal{P} \ll 1$) and when Landau levels are overlapping ($\lambda \ll 1$).

To date, MIROs have been observed in three kinds of material systems, namely, GaAs/AlGaAs [1,2], Ge/SiGe [4,5], and MgZnO/ZnO [3] heterostructures, and the dependence on ϵ, $\delta\rho_\omega \propto -\epsilon\lambda^2 \sin 2\pi\epsilon$, has been verified in many experiments. In addition, it was established that while MIROs at high microwave power significantly deviate from Eq. (1), they can still be well described within the same theoretical framework after generalization to an arbitrary radiation intensity [10,20,21]. At the same time, experiments also revealed situations when existing theory is inadequate, e.g., in describing the measured dependencies on radiation polarization [15,22] and on temperature [23]. Limitations of the theory were also identified in the regime of separated Landau levels [24] and in the radiation-induced modification of Shubnikov–de Haas oscillations [25].

One important parameter, whose role has remained largely unexplored, is the carrier density n_e. While it has been recently demonstrated that n_e affects ϵ, presumably through interaction-induced renormalization of the effective mass $m^\star$ [26,27], it should also modify other quantities, e.g., $\mathcal{P}$ and η, entering Eq. (1). Since the density dependencies of $\mathcal{P}$ and η are both known theoretically, MIRO measurements as a function of n_e should provide an important test to existing microscopic description of microwave photoresistance.

In this Rapid Communication we investigate the effect of the carrier density on the MIRO amplitude employing a tunable-density 2DEG [27–30]. We find that the quantum lifetime depends on the carrier density only weakly, in agreement with the recent study investigating Shubnikov–de Haas oscillations in a similar device [30]. Our main finding, however, is a significant *growth* of the MIRO amplitude with the carrier density. The analysis shows that this growth cannot be accounted for by the anticipated density dependence of $\mathcal{P}\eta$ entering the prefactor of Eq. (1) [17–19,31,32]. Furthermore, we find that the fundamental extrema move towards $\epsilon = 1$ which also contradicts theoretical expectations. Both of these findings indicate that our understanding of the role of density in microwave photoresistance remains limited, calling for further investigations.

Our 2DEG resides in a 30-nm GaAs/AlGaAs quantum well located about 200 nm below the sample surface. The structure is doped in a 2-nm GaAs quantum well at a setback of 63 nm on a top side. The *in situ* back gate consists of an n^+ GaAs layer situated 850 nm below the bottom of the

*Corresponding author: zudov001@umn.edu
†Present address: Microsoft Station-Q at Delft University of Technology, 2600 GA Delft, The Netherlands.

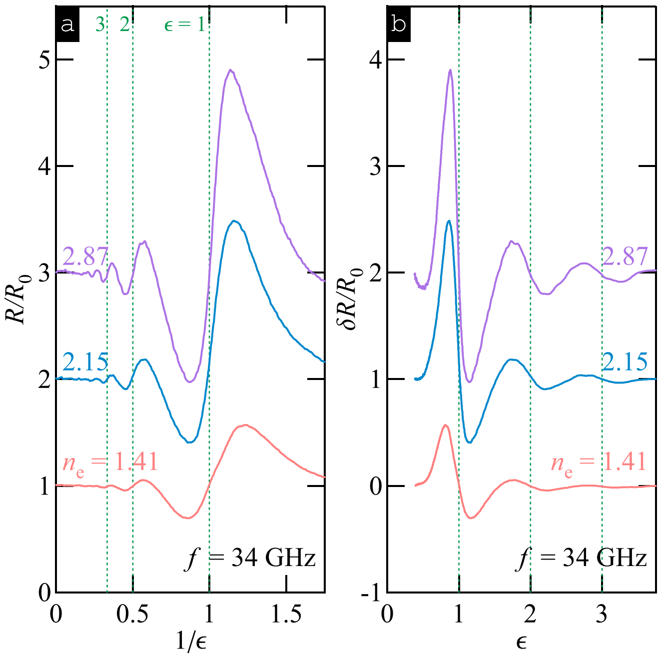

FIG. 1. (a) R/R_0 vs $1/\epsilon$ [36] at density $n_e \approx 1.41$ (bottom trace), 2.15 (middle trace), and 2.87×10^{11} cm^{-2} (top trace) at $T = 1.5$ K under irradiation by microwaves of $f = 34$ GHz. Vertical lines are drawn at $\epsilon = 1, 2, 3$, as marked. (b) $\delta R/R_0$ vs ϵ under the same conditions as in (a). The traces are vertically offset for clarity by 1.

quantum well. Ohmic contacts were fabricated at the corners and midsides of the lithographically defined 1×1 mm^2 van der Pauw mesa. The density of the 2DEG was varied from $n_e \approx 1.41$ to 2.87×10^{11} cm^{-2}. Over this density range, the low-temperature electron mobility increased from $\mu \approx 0.37$ to $\mu \approx 1.1 \times 10^7$ cm^2 V^{-1} s^{-1} [33], roughly following $\mu \propto n_e^\alpha$, with $\alpha \approx 1.5$ [34,35]. Microwave radiation, generated by a synthesized sweeper, was delivered to the sample immersed in liquid ^{3}He via a rectangular (WR-28) stainless steel waveguide. The resistance R was measured using a standard low-frequency (a few Hz) lock-in technique.

In Fig. 1(a) we present R/R_0 vs $1/\epsilon$ for three different densities, $n_e \approx 1.41$ (bottom trace), 2.15 (middle trace), and 2.87×10^{11} cm^{-2} (top trace), measured at $T = 1.5$ K under irradiation by microwaves of $f = 34$ GHz. The data show that MIROs become significantly stronger with increasing density. We next extract the oscillatory correction $\delta R/R_0$ and present the result in Fig. 1(b) as a function of ϵ. All three data sets reveal an expected periodicity with ϵ, in agreement with Eq. (1).

According to Eq. (1), the MIRO amplitude is proportional to the effective microwave power, which was shown to be [31,37]

$$\mathcal{P}(\epsilon) = \frac{\mathcal{P}^0}{2}\sum_{\pm}\frac{1}{(1 \pm \epsilon^{-1})^2 + \beta_\omega^2}, \quad \mathcal{P}^0 = \frac{e^2\mathcal{E}_{ac}^2 v_F^2}{\epsilon_{eff}\hbar^2\omega^4}. \quad (2)$$

Here, $\beta_\omega \equiv (\omega\tau_{em})^{-1} + (\omega\tau)^{-1}$, $\tau = (m^\star/e)\mu$ is the momentum relaxation time, $\tau_{em}^{-1} = n_e e^2/2\sqrt{\epsilon_{eff}}\epsilon_0 m^\star c$ [37] is the radiative decay rate, $2\sqrt{\epsilon_{eff}} = \sqrt{\varepsilon} + 1$ defines the effective dielectric constant ϵ_{eff}, $\varepsilon = 12.8$ is the dielectric constant of GaAs, v_F is the Fermi velocity, and $\mathcal{E}_{ac}$ is the microwave

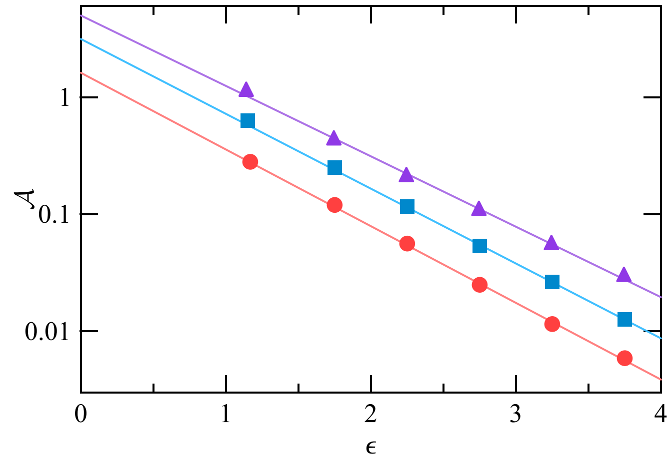

FIG. 2. $\mathcal{A} = |\delta R|_{max}/2\pi\epsilon\mathcal{P}R_0$ [38] vs ϵ for $n_e \approx 1.41$ (circles), 2.15 (squares), and 2.87×10^{11} cm^{-2} (triangles) measured at $T = 1.5$ and $f = 34$ GHz. Fits to the data with $\mathcal{A}_0 \exp(-\epsilon/f\tau_q)$ (solid lines) yield $\tau_q \approx 19.5$, 20.0, and 21.2 ps, respectively.

electric field. The density dependence of β_ω has been recently verified in time-resolved measurements of the cyclotron resonance [32]. Within the density range studied in our experiment, $\tau \gg \tau_{em}$ and $\beta_\omega \approx (\omega\tau_{em})^{-1} \propto n_e$. However, β_ω remains much smaller than unity and, as a result, $\mathcal{P}$ increases with n_e for all ϵ except in close proximity to $\epsilon = 1$. We will see, however, that the anticipated increase in $\mathcal{P}$ is rather small and contributes little to the growth of MIRO shown in Fig. 1.

The growth of MIRO with n_e observed in Fig. 1 can, in principle, stem from τ_q (entering λ) or η. Both of these parameters are readily available from the Dingle analysis. Following Eq. (1), we introduce a reduced MIRO amplitude $\mathcal{A} = |\delta R|_{max}/2\pi\epsilon\mathcal{P}R_0$ [38], where $|\delta R|_{max}$ is the MIRO amplitude, and present it in Fig. 2 as a function of ϵ for $n_e = 1.41$ (circles), 2.15 (squares), and 2.87×10^{11} cm^{-2} (triangles). Fits to the data with $\mathcal{A}_0 \exp(-\epsilon/f\tau_q)$ (solid lines) yield $\tau_q \approx 19.5$, 20.0, and 21.2 ps, respectively, indicating a slight increase of τ_q with n_e. In contrast, the intercept of the Dingle plots, $\mathcal{A}_0$, grows substantially with n_e. As we show below, theory predicts that under our experimental conditions $\mathcal{A}_0$ can only decrease with n_e.

After repeating the Dingle analysis for other n_e, we present the density dependence of τ_q (circles) in Fig. 3. A slight increase of τ_q with n_e appears to contradict a recent study [30], which has found a saturation of τ_q at $n_e \approx 2 \times 10^{11}$ cm^{-2} and a monotonic decrease at higher n_e. This discrepancy can be alleviated by recalling that Shubnikov–de Haas oscillations employed in Ref. [30] yield only impurity contributions to the quantum lifetime τ_{q0} [39,40]. The quantum lifetime obtained from MIROs, on the other hand, is reduced by electron-electron scattering. More specifically [18,41–45],

$$\frac{1}{\tau_q} = \frac{1}{\tau_{q0}} + \frac{1}{\tau_{ee}}. \quad (3)$$

Under the conditions of our experiment the electron-electron scattering rate is given by [17,41,42]

$$\frac{\hbar}{\tau_{ee}} = \frac{\pi k_B^2 T^2}{4E_F}\ln\frac{2\hbar v_F/a_B}{\pi k_B T}, \quad (4)$$

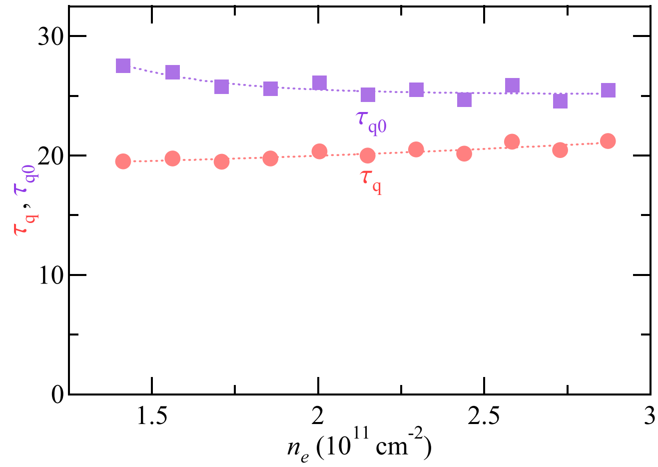

FIG. 3. τ_q (circles), obtained from the fits (cf. Fig. 2), and τ_{q0} (squares), calculated using Eqs. (3) and (4), vs n_e. The dotted lines are guides to the eye.

where E_F is the Fermi energy and $a_B \approx 11$ nm is the Bohr radius in GaAs. Using Eqs. (3) and (4) we compute τ_{q0} and present the results (squares) in Fig. 3. The results show that the impurity-limited quantum lifetime decreases slightly with n_e, in general agreement with [30]. We note, however, that in our experiment most of this decrease takes place at densities below $\approx 2 \times 10^{11}$ cm^{-2}.

As already mentioned, Fig. 2 also reveals a significant increase of the intercept of the Dingle fits, given by $\mathcal{A}_0$, with increasing n_e. Since $\mathcal{A}_0 \propto \eta$ [46], this increase reflects the increase in η, provided that the density dependence of $\mathcal{P}$ is accurately described by Eq. (2). To quantify this increase we introduce a parameter $\kappa = \mathcal{A}_0(n_e)/\mathcal{A}_0(n_l)$, where $n_l = 1.41 \times 10^{11}$ cm^{-2} is the lowest density studied. As shown in Fig. 4, κ (circles) increases by a factor of about 3 over the investigated density range. This finding is unexpected since, as we show next, one should anticipate a *decrease* of η with increasing n_e.

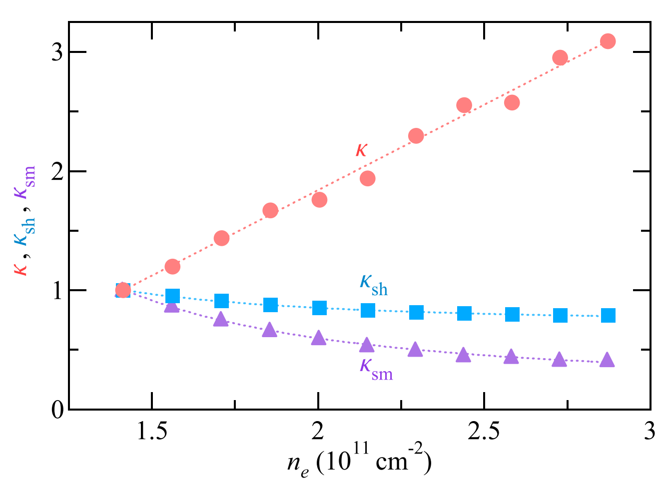

FIG. 4. κ (circles), obtained from the fits (cf. Fig. 2), κ_{sh} (squares), and κ_{sm} (triangles), calculated using Eq. (5) in the sharp and smooth disorder limit, respectively, vs n_e. The dotted lines are guides to the eye.

The dimensionless scattering rate η is given by [18]

$$\eta = \frac{\tau}{2\tau_\star} + \frac{2\tau_{in}}{\tau}, \tag{5}$$

where the first (second) term represents displacement [47–49] (inelastic [17,18]) contribution. Here, $\tau_{in} \approx 0.82\tau_{ee}$ [17] and $\tau/2\tau_\star$ [50] can vary between $\tau/2\tau_\star = 6(\tau/\tau_{q0} + 3)^{-1}$ (smooth disorder limit) and $\tau/2\tau_\star = 3/2$ (sharp disorder limit) according to the mixed-disorder model [18,51]. As a result, the relative change in η (or $\mathcal{A}_0$) with n_e is expected to fall between κ_{sm} and κ_{sh}, given by $\eta(n_e)/\eta(n_l)$ evaluated in the smooth and the sharp disorder limit, respectively. On a qualitative level, the decrease of $\tau/2\tau_\star$ with n_e can be expected whenever $\tau_q/\tau \ll 1$, i.e., when small angle scattering dominates, which is the case for all modern high-mobility GaAs quantum wells. This decrease should occur because $\tau_\star^{-1}$ [50] is less sensitive to small-angle scattering than τ^{-1} and because the characteristic scattering angle decreases with density.

As shown in Fig. 4, both κ_{sh} (squares) and κ_{sm} (triangles) monotonically decrease with n_e. The decrease in κ_{sh} with n_e occurs solely due to the weakening of the inelastic contribution, given by the second term in Eq. (5). This weakening, in turn, is due to a superlinear increase in the momentum relaxation time τ, which wins over the slightly sublinear increase in τ_{in} [see Eq. (4)]. In the smooth disorder limit, characterized by κ_{sm}, the decrease becomes larger due to the growing ratio of τ/τ_{q0} which enters the denominator of the displacement contribution [first term in Eq. (5)]. We thus conclude that regardless of the exact disorder characteristics, theoretical predictions are in contrast with the experimentally obtained κ (circles) which shows a significant *increase* over the density range studied [52]. Our findings were confirmed by measurements using $f = 39.5$ GHz in another sample which are discussed in Supplemental Material [53].

We next examine the effect of density on the positions of the MIRO extrema near the cyclotron resonance. As noted from the data in Fig. 1(b), these extrema move closer towards $\epsilon = 1$ with increasing density. To examine this behavior quantitatively, we introduce a parameter $\varphi = (\epsilon^- - \epsilon^+)/2$, where ϵ^- (ϵ^+) is the position of the fundamental minimum (maximum). We then present obtained φ (circles) in Fig. 5(a) as a function of n_e and observe that it monotonically *decreases* with n_e. Similar to τ_{q0}, the decrease is more pronounced at lower densities. Theory, however, predicts just the opposite behavior; as illustrated in Fig. 5(a), the calculated values of φ_{sh} (squares) and φ_{sm} (triangles), representing sharp and smooth disorder limits, respectively, both increase with n_e. The expected growth of $\varphi_{sh} \approx \varphi_{sm}$ with n_e occurs, for the most part, due to the increase in β_ω, dominated by $\tau_{em}^{-1} \propto n_e$, which controls the sharpness of $\mathcal{P}$ near $\epsilon = 1$. Indeed, as shown in Fig. 5(b), $\mathcal{P}(\epsilon)$ is considerably sharper at $n_e = 1.41 \times 10^{11}$ cm^{-2} (solid line) than at $n_e = 2.87 \times 10^{11}$ cm^{-2} (dotted line).

It is known that the phase reduction can occur with increasing $\mathcal{P}$ due to contributions from multiphoton processes [20,21]. This scenario, however, can be ruled out since $\mathcal{P}$, in fact, decreases with n_e near $\epsilon = 1$ within the investigated density range. As shown in Fig. 5(c), $\mathcal{P}$ at the fundamental MIRO extrema (solid and open circles) exhibits a slight overall decrease within the studied density range, similar to $\mathcal{P}$ at

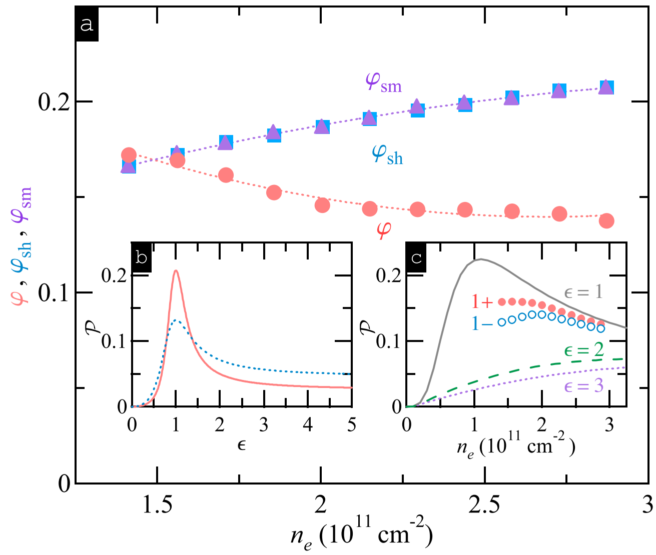

FIG. 5. (a) φ (circles), φ_{sh} (squares), and φ_{sm} (triangles) vs n_e. The dotted lines are guides to the eye. (b) $\mathcal{P}$ [38] vs ϵ for $n_e = 1.41 \times 10^{11}$ cm^{-2} (solid line) and $n_e = 2.87 \times 10^{11}$ cm^{-2} (dotted line). (c) $\mathcal{P}$ [38] vs n_e for $\epsilon = 1$ (solid line), $\epsilon = 2$ (dashed line), and $\epsilon = 3$ (dotted line). Also shown is $\mathcal{P}$ vs n_e at the first MIRO maximum (1+, solid circles) and minimum (1−, open circles).

$\epsilon = 1$ (solid line). At higher MIRO orders, $\mathcal{P}$ monotonically increases, as illustrated by dashed and dotted lines computed for $\epsilon = 2$ and $\epsilon = 3$, respectively. This increase in $\mathcal{P}$ occurs because $\mathcal{P}_0 \propto n_e$ while β_ω remains relatively small within the studied density range.

One somewhat uncertain parameter is ϵ_{eff} which affects β_ω entering $\mathcal{P}$ given by Eq. (2). Indeed, the expression we have used is generally valid only when the overall sample thickness greatly exceeds the radiation wavelength, a condition which is not satisfied for the microwave frequency used in our experiment. According to Ref. [19], a better approximation would be using $\epsilon_{\text{eff}} = 1$ which would increase the value of β_ω by approximately a factor of 2. However, any increase in β_ω would only weaken (or even reverse) the density dependence of $\mathcal{P}$ and further increase the disagreement between theory and experiment, both in η and φ.

Finally, we note that by applying the gate voltage we are not only changing the carrier density but also modifying the confinement potential. Numerical simulations show that the 2DEG is pulled away from the top interface towards the center of the quantum well and becomes wider with increasing density. Whether or not such a change of the confinement plays any significant role in the observed enhancement of the MIRO amplitude is unclear at this point and is left for future studies. To investigate this possibility, it would be interesting to perform measurements in different structures, such as heterojunction-insulated gate field-effect transistors, in which confinement becomes stronger with increasing carrier density.

In summary, we have investigated the effect of the carrier density n_e on the MIRO amplitude in a high-mobility modulation-doped GaAs/AlGaAs quantum well equipped with an *in situ* back gate. Our main finding is a significant *growth* of the MIRO amplitude with increasing density. A Dingle analysis shows that this increase originates primarily from $\mathcal{P}\eta$ entering Eq. (1) and not from a slight increase of τ_q. This finding is in conflict with theoretical expectations which predict a modest increase of $\mathcal{P}$ and a *decrease* of η with increasing density. We further find that the MIRO extrema near the cyclotron resonance move toward each other with increasing n_e whereas the theory predicts just the opposite behavior. These findings indicate that our understanding of microwave photoresistance is still lacking and needs further examination.

We thank Q. Shi and Q. Ebner for assistance with experiments and M. Sammon for discussions. The work at Minnesota was supported by the NSF Award No. DMR-1309578 (experiments discussed in the main text) and by the U.S. Department of Energy, Office of Science, Basic Energy Sciences, under Award No. ER 46640-SC0002567 (complementary experiments discussed in Supplemental Material). The work at Purdue was supported by the U.S. Department of Energy, Office of Science, Basic Energy Sciences, under Award No. DE-SC0006671.

[1] M. A. Zudov, R. R. Du, J. A. Simmons, and J. L. Reno, Phys. Rev. B **64**, 201311(R) (2001).
[2] P. D. Ye, L. W. Engel, D. C. Tsui, J. A. Simmons, J. R. Wendt, G. A. Vawter, and J. L. Reno, Appl. Phys. Lett. **79**, 2193 (2001).
[3] D. F. Kärcher, A. V. Shchepetilnikov, Y. A. Nefyodov, J. Falson, I. A. Dmitriev, Y. Kozuka, D. Maryenko, A. Tsukazaki, S. I. Dorozhkin, I. V. Kukushkin *et al.*, Phys. Rev. B **93**, 041410 (2016).
[4] M. A. Zudov, O. A. Mironov, Q. A. Ebner, P. D. Martin, Q. Shi, and D. R. Leadley, Phys. Rev. B **89**, 125401 (2014).
[5] Q. Shi, Q. A. Ebner, and M. A. Zudov, Phys. Rev. B **90**, 161301(R) (2014).
[6] W. Zhang, M. A. Zudov, L. N. Pfeiffer, and K. W. West, Phys. Rev. Lett. **98**, 106804 (2007).
[7] A. T. Hatke, H.-S. Chiang, M. A. Zudov, L. N. Pfeiffer, and K. W. West, Phys. Rev. B **77**, 201304(R) (2008).
[8] A. T. Hatke, H.-S. Chiang, M. A. Zudov, L. N. Pfeiffer, and K. W. West, Phys. Rev. Lett. **101**, 246811 (2008).
[9] A. A. Bykov, I. V. Marchishin, A. V. Goran, and D. V. Dmitriev, Appl. Phys. Lett. **97**, 082107 (2010).
[10] M. Khodas, H. S. Chiang, A. T. Hatke, M. A. Zudov, M. G. Vavilov, L. N. Pfeiffer, and K. W. West, Phys. Rev. Lett. **104**, 206801 (2010).
[11] O. M. Fedorych, M. Potemski, S. A. Studenikin, J. A. Gupta, Z. R. Wasilewski, and I. A. Dmitriev, Phys. Rev. B **81**, 201302 (2010).
[12] I. V. Andreev, V. M. Muravev, I. V. Kukushkin, S. Schmult, and W. Dietsche, Phys. Rev. B **83**, 121308(R) (2011).
[13] A. D. Levin, Z. S. Momtaz, G. M. Gusev, O. E. Raichev, and A. K. Bakarov, Phys. Rev. Lett. **115**, 206801 (2015).
[14] S. I. Dorozhkin, A. A. Kapustin, V. Umansky, K. von Klitzing, and J. H. Smet, Phys. Rev. Lett. **117**, 176801 (2016).

[15] T. Herrmann, I. A. Dmitriev, D. A. Kozlov, M. Schneider, B. Jentzsch, Z. D. Kvon, P. Olbrich, V. V. Bel'kov, A. Bayer, D. Schuh *et al.*, Phys. Rev. B **94**, 081301(R) (2016).

[16] T. Herrmann, Z. D. Kvon, I. A. Dmitriev, D. A. Kozlov, B. Jentzsch, M. Schneider, L. Schell, V. V. Bel'kov, A. Bayer, D. Schuh *et al.*, Phys. Rev. B **96**, 115449 (2017).

[17] I. A. Dmitriev, M. G. Vavilov, I. L. Aleiner, A. D. Mirlin, and D. G. Polyakov, Phys. Rev. B **71**, 115316 (2005).

[18] I. A. Dmitriev, M. Khodas, A. D. Mirlin, D. G. Polyakov, and M. G. Vavilov, Phys. Rev. B **80**, 165327 (2009).

[19] I. A. Dmitriev, A. D. Mirlin, D. G. Polyakov, and M. A. Zudov, Rev. Mod. Phys. **84**, 1709 (2012).

[20] A. T. Hatke, M. Khodas, M. A. Zudov, L. N. Pfeiffer, and K. W. West, Phys. Rev. B **84**, 241302(R) (2011).

[21] Q. Shi, M. A. Zudov, I. A. Dmitriev, K. W. Baldwin, L. N. Pfeiffer, and K. W. West, Phys. Rev. B **95**, 041403(R) (2017).

[22] J. H. Smet, B. Gorshunov, C. Jiang, L. Pfeiffer, K. West, V. Umansky, M. Dressel, R. Meisels, F. Kuchar, and K. von Klitzing, Phys. Rev. Lett. **95**, 116804 (2005).

[23] Q. Shi, S. A. Studenikin, M. A. Zudov, K. W. Baldwin, L. N. Pfeiffer, and K. W. West, Phys. Rev. B **93**, 121305(R) (2016).

[24] A. T. Hatke, M. A. Zudov, L. N. Pfeiffer, and K. W. West, Phys. Rev. B **84**, 241304(R) (2011).

[25] Q. Shi, P. D. Martin, A. T. Hatke, M. A. Zudov, J. D. Watson, G. C. Gardner, M. J. Manfra, L. N. Pfeiffer, and K. W. West, Phys. Rev. B **92**, 081405(R) (2015).

[26] A. V. Shchepetilnikov, D. D. Frolov, Y. A. Nefyodov, I. V. Kukushkin, and S. Schmult, Phys. Rev. B **95**, 161305 (2017).

[27] X. Fu, Q. A. Ebner, Q. Shi, M. A. Zudov, Q. Qian, J. D. Watson, and M. J. Manfra, Phys. Rev. B **95**, 235415 (2017).

[28] J. D. Watson, G. A. Csáthy, and M. J. Manfra, Phys. Rev. Appl. **3**, 064004 (2015).

[29] Q. Shi, M. A. Zudov, Q. Qian, J. D. Watson, and M. J. Manfra, Phys. Rev. B **95**, 161303(R) (2017).

[30] Q. Qian, J. Nakamura, S. Fallahi, G. C. Gardner, J. D. Watson, S. Lüscher, J. A. Folk, G. A. Csáthy, and M. J. Manfra, Phys. Rev. B **96**, 035309 (2017).

[31] M. Khodas and M. G. Vavilov, Phys. Rev. B **78**, 245319 (2008).

[32] Q. Zhang, T. Arikawa, E. Kato, J. L. Reno, W. Pan, J. D. Watson, M. J. Manfra, M. A. Zudov, M. Tokman, M. Erukhimova *et al.*, Phys. Rev. Lett. **113**, 047601 (2014).

[33] Mobility values were estimated using the standard van der Pauw method. The zero-field resistance anisotropy ratio in our samples was found to be less than 2.

[34] The obtained value of α is in agreement with recent theoretical calculations [35] considering GaAs quantum wells similar to the one employed in our study.

[35] M. Sammon, M. A. Zudov, and B. I. Shklovskii, Phys. Rev. Mater. **2**, 064604 (2018).

[36] ϵ was computed using $m^\star = 0.0652, 0.0638$, and $0.0631 m_0$ for $n_e = 1.41, 2.15$, and 2.87×10^{11} cm^{-2}, respectively [27].

[37] K. W. Chiu, T. K. Lee, and J. J. Quinn, Surf. Sci. **58**, 182 (1976).

[38] $\mathcal{P}$ was calculated using Eq. (2) with $\mathcal{E}_{ac} = 1$ V/cm and $m^\star = 0.067 m_0$ entering ϵ and τ_{em}.

[39] G. W. Martin, D. L. Maslov, and M. Y. Reizer, Phys. Rev. B **68**, 241309 (2003).

[40] Y. Adamov, I. V. Gornyi, and A. D. Mirlin, Phys. Rev. B **73**, 045426 (2006).

[41] A. V. Chaplik, Zh. Eksp. Teor. Fiz. **60**, 1845 (1971) [Sov. Phys. JETP **33**, 997 (1971)].

[42] G. F. Giuliani and J. J. Quinn, Phys. Rev. B **26**, 4421 (1982).

[43] V. Ryzhii and R. Suris, J. Phys.: Condens. Matter **15**, 6855 (2003).

[44] V. Ryzhii, A. Chaplik, and R. Suris, JETP Lett. **80**, 363 (2004).

[45] A. T. Hatke, M. A. Zudov, L. N. Pfeiffer, and K. W. West, Phys. Rev. Lett. **102**, 066804 (2009).

[46] Microwave power is not exactly known and $\mathcal{A}_0$ differs from η by a numerical factor.

[47] A. C. Durst, S. Sachdev, N. Read, and S. M. Girvin, Phys. Rev. Lett. **91**, 086803 (2003).

[48] X. L. Lei and S. Y. Liu, Phys. Rev. Lett. **91**, 226805 (2003).

[49] M. G. Vavilov and I. L. Aleiner, Phys. Rev. B **69**, 035303 (2004).

[50] The rate of scattering on angle θ can be expressed in terms of angular harmonics, $\tau_n = \tau_{-n}$, as $\tau_\theta^{-1} = \sum_{-\infty}^{+\infty} \tau_n^{-1} e^{in\theta}$. In this notation, $\tau_{q0}^{-1} \equiv \langle \tau_\theta^{-1} \rangle_\theta = \tau_0^{-1}$, $\tau^{-1} \equiv \langle \tau_\theta^{-1}(1-\cos\theta)\rangle_\theta = \tau_0^{-1} - \tau_1^{-1}$, and $\tau_\star^{-1} \equiv 2\langle \tau_\theta^{-1}(1-\cos\theta)^2\rangle_\theta = 3\tau_0^{-1} - 4\tau_1^{-1} + \tau_2^{-1}$ ($\langle \cdots \rangle_\theta$ denotes averaging over θ). In the mixed disorder model [51], $\tau_n^{-1} = \tau_{sh}^{-1}\delta_{n,0} + \tau_{sm}^{-1}(1+\chi n^2)^{-1}$, where τ_{sh}^{-1} and τ_{sm}^{-1} represent, respectively, scattering rates for background impurities and remote ionized donors [located at a distance d from the interface, $\chi = (2k_F d)^{-2}$].

[51] M. G. Vavilov, I. L. Aleiner, and L. I. Glazman, Phys. Rev. B **76**, 115331 (2007).

[52] An alternative theoretical proposal [54] considering MIROs in terms of classical memory effects for the case of small-angle scattering predicts $\eta \propto \tau n_e^{1/2}$. We note, however, that the inelastic mechanism was not considered in Ref. [54] and that their choice of the disorder potential predicts $\tau_q, \tau \propto n_e^{-1/2}$ leading to density-independent η.

[53] See Supplemental Material at http://link.aps.org/supplemental/10.1103/PhysRevB.98.121303 for additional data obtained in a different sample using microwave frequency of f = 39.5 GHz.

[54] Y. M. Beltukov and M. I. Dyakonov, Phys. Rev. Lett. **116**, 176801 (2016).